JOURNAL OF SOLID STATE CHEMISTRY 11, 120–127 (1974)

A Thermodynamic Study of Iron in Reduced Rutile

I. E. GREY, C. LI, AND A. F. REID

Division of Mineral Chemistry, CSIRO, P.O. Box 124, Port Melbourne, Victoria 3207, Australia

Received November 21, 1973

Oxygen activity–composition isotherms at 1473°K have been established for the Ti–O and Fe–Ti–O systems in the composition range $MO_{1.667}$–$MO_{1.875}$, i.e., for the reduced rutile Magnéli phases M_nO_{2n-1}, $n = 3$–8, M = Fe,Ti. The quenching method was used and control of oxygen activity achieved with CO_2/H_2 mixtures. Marked hysteresis was observed in the Ti–O system as well as reproducible bivariant behaviour in the two phase regions. These effects were reduced considerably in the Fe–Ti–O system. A partial representation of the Fe–Ti–O ternary composition diagram at 1473°K has been established. The Magnéli phases incorporate about 1 at.% of divalent iron in solid solutions of the type Ti_nO_{2n-1}–$FeTi_{n-1}O_{2n-1}$. The relevance of the thermodynamic data to an ilmenite upgrading process is discussed.

1. Introduction

A knowledge of the extent of incorporation of iron into reduced rutile phases is of interest in determining the stabilization of Fe^{2+} in the presence of Ti^{3+}, and is of industrial importance in relation to ilmenite upgrading. In ilmenite beneficiation processes which involve reduction of the iron content to metal at subslagging temperatures (*1*, *2*) the final reduction product consists mainly of metallic iron plus reduced rutiles (*3*). After extraction of the metallic iron, the purity of the final titanium oxide product is limited by its solubility for iron, as Fe^{2+} (*4*). The extension of the solid solutions of the phases TiO_{2-x} towards their ferrous iron counterparts, $Fe_yTi_{1-y}O_{2-x}$, in the Fe–Ti–O system is a function of temperature, oxygen activity, and composition. Thermodynamic studies on this part of the Fe–Ti–O ternary system do not appear to have been reported, although there have been numerous publications dealing with reduced rutile phases in the Ti–O binary system (*5–11*).

We report here the results of a thermodynamic study at 1473°K of the incorporation of iron into reduced rutile phases with compositions MO_{2-x}(M = Fe,Ti) where $0.125 \leqslant x \leqslant 0.333$.

2. Experimental

2.1. General Procedure

The phases at equilibrium at 1473°K in the reduced rutile region of the Fe–Ti–O system were determined by the quenching technique. Suitable mixtures of Fe_2O_3 and TiO_2 were equilibrated at a controlled oxygen activity for 16–24 hr, then rapidly quenched with liquid nitrogen. The phases present were determined by the X-ray diffraction method. The compositions of the reduced rutile phases in equilibrium with metallic iron were determined by chemical analysis and by a magnetic susceptibility method (see Section 2.4). Fisher Certified reagent ferric oxide and titanium dioxide (anatase) were used as starting materials after being dried at 1000°K for 2 days.

2.2. Apparatus

The quench runs were made in a horizontal platinum-wound furnace. Temperature stability to ±0.5°K was maintained with an Ether "Transitrol" potentiometric controller, and

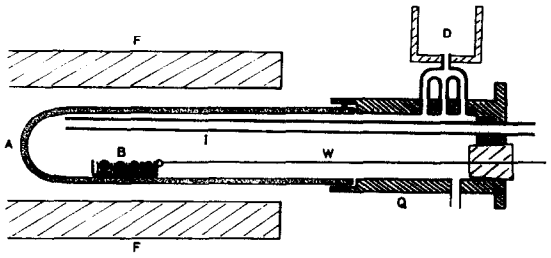

FIG. 1. Horizontal quench furnace used in this study. A, alumina work tube; B, molybdenum boat; F, horizontal platinum furnace; I, gas inlet tube; D, polystyrene funnel for liquid nitrogen; Q, brass quench end; W, molybdenum draw wire.

temperatures were measured with a thermocouple, calibrated to an accuracy of ±1°K.

The sample pellets were held in a boat made from molybdenum sheet. Equilibration runs were made in a closed end Alsint (recrystallized alumina) tube fitted with a water-cooled brass quench end (Fig. 1). The design, similar to that described by Webster and Bright (*12*) allows efficient preheating of the atmosphere control gas mixture by passage through a preheating tube followed by contact with the rounded closed end of the work tube. A molybdenum draw wire attached to the molybdenum boat was used to rapidly withdraw the boat into the brass quench end, where the samples were immersed in liquid nitrogen introduced through the ports shown schematically in Fig. 1. This procedure resulted in very rapid quenching.

2.3. *Control of Atmosphere*

Controlled atmospheres were obtained by mixing carbon dioxide and hydrogen in specific ratios by use of differential flow-meters as described by Darken and Gurry (*13*). The apparatus included constant pressure inlet regulators for each gas, mercury manometers for adjustment of pressure drop across precision flowmeters, a packed bed mixing chamber, and a final flowmeter to monitor total flow rates which were sufficiently high to avoid thermal diffusion effects. The analytical grade carbon dioxide had a purity of 99.99% ($H_2O < 30$ ppm; air < 100 ppm) and the hydrogen a purity of 99.995% ($H_2O < 23$ ppm; air < 10 ppm). The hydrogen was further purified by passage through first a column of B.T.S. catalyser (active copper on an alumina substrate) and then through a column of predried molecular sieves. With hydrogen purified by this treatment it was possible at 1473°K to reduce TiO_2 to Ti_2O_3, indicating an effective oxygen activity of less than 10^{-18}.

2.4. *Determination of Phase Boundaries*

The compositions of reduced rutile phases MO_{2-x}, $0.125 \leqslant x \leqslant 0.333$, i.e., the Magnéli phases (*14*), in equilibrium with metallic iron were determined very precisely by means of magnetic susceptibility measurements on the quenched samples. We found that when care was taken in the preparation of uniform samples, the gramme susceptibility of standard mixtures of paramagnetic compounds plus metallic iron was a linear function of the wt% of iron present within the range 0–5 wt% of metallic iron.

In the two-phase reduced rutile plus iron regions of the Fe–Ti–O phase diagram, compositions which lie on a particular tie line of constant oxygen activity consist of different relative amounts of metallic iron and the equilibrium reduced rutile phase. Our method of determining the phase boundary involved the simultaneous equilibration of up to 5 samples with different iron/titanium ratios at a chosen oxygen activity. The products were quenched and the phases present identified by X-ray diffraction. For those runs giving two-phase, iron plus reduced rutile products, the gramme susceptibility of each of the samples was then measured. The plots of gramme susceptibility vs the Fe/Ti ratio were linear, and the intercept on

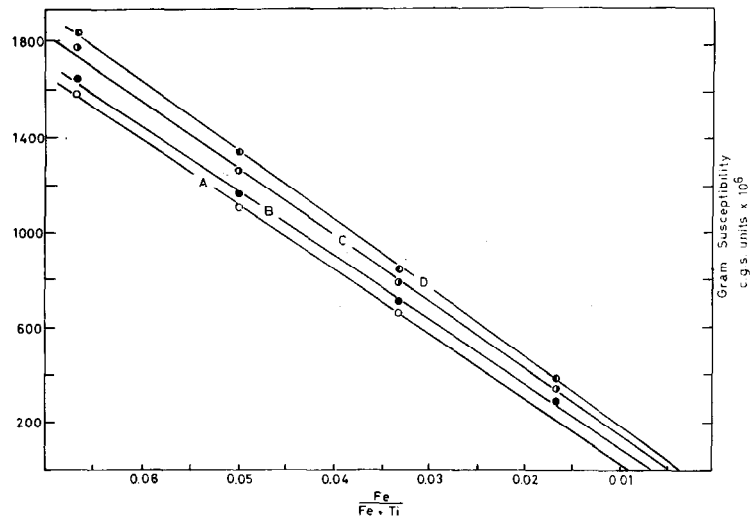

FIG. 2. Gramme susceptibility–composition curves for M_4O_7 plus metallic iron at 4 different oxygen activities, A, $a_{O_2} = 10^{-15.85}$; B, $a_{O_2} = 10^{-15.95}$; C, $a_{O_2} = 10^{-16.25}$, D, $a_{O_2} = 10^{-16.40}$.

the composition axis gave a precise determination of the atomic fraction of iron in the reduced rutile. Typical results are illustrated in Fig. 2. The atomic fraction of iron incorporated in the reduced rutile phases, as a function of oxygen activity, was also determined from chemical analysis.

2.5. *Chemical Analysis*

Equilibrium products were analysed for metallic iron, ferrous iron and total reducibles, Fe(II) plus Ti(III).

Metallic iron was extracted and determined by a reflux leaching procedure using an anhydrous bromine–methanol reagent. The residue from the extraction was divided into two parts. The first part was dissolved in a hydrofluoric–sulphuric acid solution containing excess pentavalent vanadium, enclosed in a Teflon bomb at 470°K. The combined Fe(II) + Ti(III) content was determined by back titration of the excess vanadium(V) content with standard ferrous sulphate solution. The remainder of the residue was dissolved in hydrofluoric acid and stannous chloride added to reduce the iron present to the divalent state. The ferrous iron was titrated against potassium dichromate. The metallic iron and ferrous iron analyses were also checked by atomic absorption spectrometry.

2.6. *Physical Measurements*

X-ray powder diffraction patterns were obtained with a Philips diffractometer fitted with a graphite monochromator and using Cu$K\alpha$ radiation. Silicon was used as an internal standard, and slow scan rates ($\frac{1}{4}$°/min) were used to ensure high precision in the data. For magnetic susceptibility measurements the Gouy method was used. To avoid too great a force being produced by the presence of metallic iron, small diameter (2 or 3 mm) sample tubes were used, and when necessary samples were uniformly diluted with a diamagnetic diluent.

3. Accuracy of Results

The phase equilibria described in this paper involve phase changes occurring over very narrow oxygen activity (a_{O_2}) ranges and very small compositional changes. For precise definition of the system a careful thermogravimetric study, *at temperature*, ideally is required. However, by observing the precautions described in Section 2, primarily rapid quenching, gas purification and efficient preheating, and by carrying out a large number of equilibrations (over 80 runs, each involving 4 or 5 different samples) we have been able to obtain meaningful, reproducible data for this

TABLE I

EXAMPLES OF DUPLICATE EQUILIBRATIONS IN THE Ti–O SYSTEM

		Equilibrium products	
		Starting material	
Run No.	Log a_{O_2}	TiO_2	Ti_2O_3
ANR 118	−15.04	Ti_8O_{15} + trace Ti_9O_{17}	Ti_8O_{15}
ANR 181	−15.05	Ti_8O_{15}	—
ANR 134	−15.07	Ti_8O_{15}	Ti_8O_{15}
ANR 135	−15.07	Ti_8O_{15}	Ti_8O_{15}
ANR 140	−15.18	Ti_8O_{15}(90)[a] + Ti_7O_{13}(10)	Ti_6O_{11}(30) + Ti_7O_{13}(70)
ANR 117	−15.20	Ti_8O_{15}(60) + Ti_7O_{13}(40)	—
ANR 170	−15.23	Ti_7O_{13}	Ti_6O_{11}
ANR 146	−15.25	Ti_7O_{13} + trace Ti_6O_{11}	Ti_6O_{11}

[a] Numbers in parentheses are approximate weight percentages of Magnéli phases estimated from a comparison of the intensities of X-ray diffraction peaks.

system using the quench method. The accuracy of the results is discussed below.

3.1. Oxygen Activity

The flowmeters were carefully calibrated by the bubble meter method (*15*) to an accuracy better than ±2%. This combined uncertainty in the CO_2 and H_2 flow rates results in a maximum uncertainty in $\log a_{O_2}$ of ±0.03. A further uncertainty in $\log a_{O_2}$ of ±0.02 results from variations in room temperature of ±1°K during the period of an equilibration run (20 hr). The combined *maximum* uncertainty in $\log a_{O_2}$ is thus ±0.05. The accuracy obtained in our experiments was actually better than this, as evidenced by the reproducibility between separate runs in which $\log a_{O_2}$ was kept almost constant (see Table I).

Hysteresis effects were studied by *simultaneously* equilibrating pairs of pellets, one being more oxidized, the other more reduced, than the equilibrium product. The variation in $\log a_{O_2}$ between such pairs of samples was a function only of the temperature gradient across the samples. The maximum variation in temperature between pairs of samples was 1.5°K, measured to a precision of ±0.2°K. This temperature variation results in a variation in $\log a_{O_2}$ of 0.02. The precision of determination of the hysteresis effect is thus 0.02 in $\log a_{O_2}$.

3.2. Compositions

It is difficult to place absolute uncertainties on analyses, where the human element is involved. Therefore an estimate of the accuracy

TABLE II

COMPARISON OF ATOMIC FRACTIONS OF IRON IN M_4O_7 AS ESTIMATED BY TWO DIFFERENT ANALYTICAL PROCEDURES

		x (atomic fraction of iron in Magnéli phase)	
Log a_{O_2}	Equilibrium products	From magnetic measurements	From chemical analyses
−15.85	$(Fe_xTi_{1-x})_4O_7$ + Fe_{metal}	0.0095 (line A, Fig. 2)	0.011
−15.95	$(Fe_xTi_{1-x})_4O_7$ + Fe_{metal}	0.0075 (line B, Fig. 2)	0.0095
−16.25	$(Fe_xTi_{1-x})_4O_7$ + Fe_{metal}	0.005 (line C, Fig. 2)	0.007
−16.40	$(Fe_xTi_{1-x})_4O_7$ + Fe_{metal}	0.004 (line D, Fig. 2)	0.005

of the determination of the atomic fraction of iron has been made by a comparison of results obtained by two entirely different methods of analysis. In Table II are compared the values obtained by both the magnetic susceptibility method and by chemical analysis, for the atomic fraction of iron, x, in $(Fe_xTi_{1-x})_4O_7$ prepared at 4 different oxygen activities. The discrepancy between the 2 sets of results lies in the range $\Delta x = 0.001$–0.002, and so the metal atomic fractions from Table III are accurate to about ± 0.002.

In this paper the M/O ratio for each of the Magnéli phases is assumed to be that given exactly by the stoichiometries M_nO_{2n-1}. In a very precise thermogravimetric study of the Ti–O system at 1303°K, Merritt observed that for the composition TiO_x, $x = 1.7500$ (i.e., Ti_4O_7), the width Δx due to nonstoichiometry in the M/O ratio was less than 0.0005 (*9*).

The accuracy of the determination of the boundary between one- and two-Magnéli phase regions was contingent upon detection of a second phase in the X-ray diffractogram of the products, i.e., 3–4% by weight.

4. Results

4.1. The TiO_{2-x} Binary System

For this binary edge of the ternary Fe–Ti–O system we have determined the oxygen

TABLE III

THERMODYNAMIC DATA FOR TI–O AND FE–TI–O AT 1473°K
INVARIANT POINTS

Ti–O		Fe–Ti–O	
Composition of phases	Oxygen activity	Composition of phases in equilibrium with iron metal	Oxygen activity
Ti_8O_{15} + Ti_7O_{13}	$10^{-15.13}$[a](oxidn) $10^{-15.18}$(redn)	$(Fe_{0.009}Ti_{0.991})_8O_{15}$ + $(Fe_{0.010}Ti_{0.990})_7O_{13}$ (Area I, Fig. 5)	$10^{-15.0}$(oxidn) $10^{-15.07}$(redn)
Ti_7O_{13} + Ti_6O_{11}	$10^{-15.18}$(oxidn) $10^{-15.3}$(redn)	$(Fe_{0.009}Ti_{0.991})_7O_{13}$ + $(Fe_{0.012}Ti_{0.988})_6O_{11}$ (Area II, Fig. 5)	$10^{-15.07}$(oxidn) $10^{-15.15}$(redn)
Ti_6O_{11} + Ti_5O_9	$10^{-15.58}$(oxidn) $10^{-15.68}$(redn)	$(Fe_{0.007}Ti_{0.993})_6O_{11}$ + $(Fe_{0.008}Ti_{0.992})_5O_9$ (Area III, Fig. 5)	$10^{-15.55}$(oxidn and redn)
Ti_5O_9 + Ti_4O_7	$10^{-15.86}$(oxidn) $10^{-15.92}$(redn)	$(Fe_{0.006}Ti_{0.994})_5O_9$ + $(Fe_{0.010}Ti_{0.990})_4O_7$ (Area IV, Fig. 5)	$10^{-15.83}$(oxidn and redn)
Ti_4O_7 + Ti_3O_5	$10^{-16.71}$[b]	$(Fe_{0.005}Ti_{0.995})_4O_7$ + $(Fe_{0.008}Ti_{0.992})_3O_5$ (Area V, Fig. 5)	

[a] Most of the two (Ti–O) and three (Fe–Ti–O) phase regions show slight but reproducible bivariant behaviour (see text). The oxygen activities given are mean values.
[b] Ref. 11.

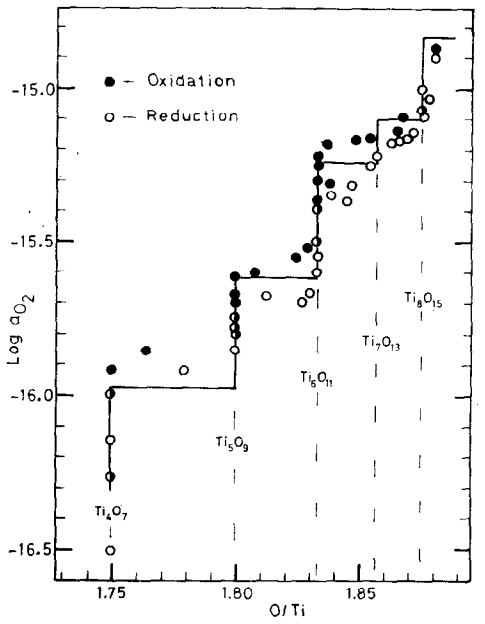

FIG. 3. Oxygen activity–composition isotherm for Ti–O at 1473°K. Solid line, Suzuki and Sambongi (*11*); all plotted points, our data (◑ = coincident points).

activity–composition relationship at 1473°K for the compositions $TiO_{1.667}(Ti_3O_5)$–$TiO_{1.875}$ (Ti_8O_{15}). The results are summarized in Table III and Fig. 3.

Equilibrium was approached by both reduction and oxidation by simultaneous equilibration of pellets of TiO_2 and Ti_2O_3. We consistently obtained a hysteresis effect; the equilibrium phase(s) obtained by oxidation had a lower O/Ti ratio than the phase(s) obtained by reduction *at the same oxygen activity*. The effect manifests itself as a series of closed loops separated by single phase regions in which the composition remains constant over a range of oxygen activities (Fig. 3). The width of the loops varies in the range 0.05–0.2 in $\log a_{O_2}$.

For both oxidation and reduction paths the range of equilibrium oxygen activities for single Magnéli phases, Ti_nO_{2n-1}, is narrower for homologues with *n*-odd than for adjacent *n*-even homologues. In fact we were unable to quench a single phase Ti_7O_{13}; a fairly smooth transition from biphasic mixtures of $Ti_6O_{11} + Ti_7O_{13}$ to mixtures of $Ti_7O_{13} + Ti_8O_{15}$ over a narrower oxygen activity range was observed. We were able, however, to obtain the higher homologue, Ti_8O_{15}, over a range of oxygen activities (Fig. 3).

4.2. *The System* $(Fe,Ti)O_{2-x} + Fe$

The equilibrium of Magnéli phases in contact with metallic iron is represented in Fig. 4, as a plot of O/M ratio (M = Fe, Ti) vs oxygen activity. In contrast to the results for the binary Ti–O system, there is virtually no hysteresis between the oxidation and reduction paths except near the Magnéli phase M_7O_{13}. As in our studies on the Ti–O system, we were unable to prepare a *completely* pure sample of M_7O_{13} in equilibrium with iron metal; there was a change from the 3 phase iron + M_6O_{11} + M_7O_{13} to 3 phase iron + M_7O_{13} + M_8O_{15} over a narrow oxygen activity range, $\Delta \log a_{O_2} < 0.05$. The oxygen activity stability range for M_5O_9 is seen from Fig. 4 and Table III to be narrower than that for the adjacent *n*-even homologues M_4O_7 and M_6O_{11}.

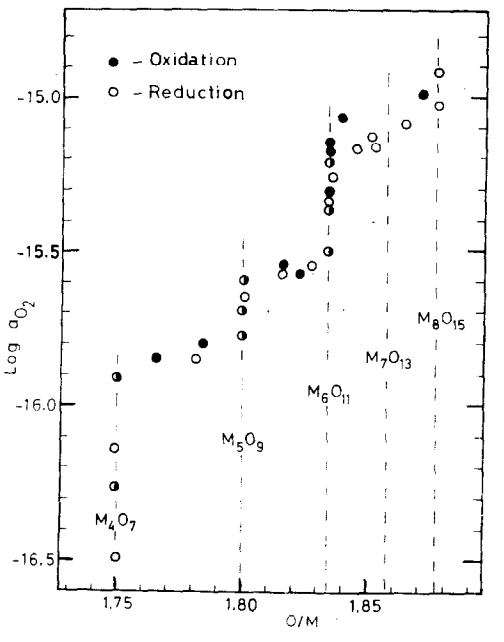

FIG. 4. Oxygen activity–composition isotherm for Fe–Ti–O at 1473°K—equilibrium of Magnéli phases with metallic iron (◑ = coincident points).

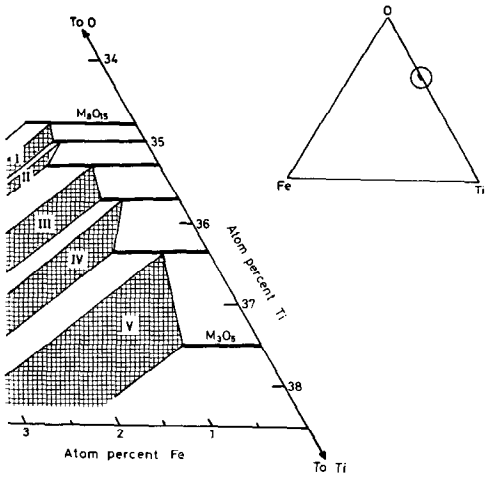

FIG. 5. Partial phase diagram for the reduced rutile region of the Fe–Ti–O phase diagram at 1473°K. Region of study is enclosed by the circle in the inset. No evidence was found for deviations from the stoichiometries M_nO_{2n-1} and so they are represented as line phases. The cross-hatched 3 phase regions I–V are described in Table III.

Within the 2 phase regions comprising a Magnéli phase plus metallic iron, the variation of the Fe/Ti ratio in the equilibrium Magnéli phase was determined as a function of oxygen activity, using the magnetic susceptibility method described in Section 2.4. Typical plots of susceptibility vs Fe/Fe + Ti ratio are shown in Fig. 2. The resulting calculated compositions for the Magnéli phases at the boundaries of the 2 and 3 phase regions are given in Table III. The results are combined to give an idealized form of the ternary composition diagram, in Fig. 5. In this diagram the Magnéli phases are shown as line phases with M/O ratios given exactly by the formulae M_nO_{2n-1}, and the bivariant behaviour is omitted.

5. Discussion

The hysteresis effect shown in Fig. 3 has previously been observed in the Ti–O system by Merritt et al. (*10*). At the lower temperature of their study, 1303°K, the hysteresis is much more severe, consisting of one large loop originating at the composition $TiO_{1.75}$ and closing at the composition $TiO_{1.90}$ with inflexions near the different Magnéli phase compositions; i.e., there is a fusion of the separate loops between pairs of adjacent Magnéli phases. The nonequilibrium implied by the hysteresis has been explained in detail by Merritt et al. The structures of adjacent Magnéli phases are very similar, and coherent intergrowth between adjacent phases, with microdomains as small as 100–200 Å, has been observed in electron microscope studies (*16*). A biphasic mixture which is *coherently* intergrown on such a fine scale behaves as a *nonstoichiometric* single phase or *pseudophase* (*17*) for which the composition varies with oxygen activity. This gives rise to bivariant behaviour as exhibited in Fig. 3. The "new phase" of composition $TiO_{1.82}$ observed by Anderson and Khan (*8*) is most likely due to bivariant behaviour in the two phase region, $Ti_5O_9 + Ti_6O_{11}$. We obtained *no* X-ray diffraction evidence for an ordered intergrowth phase in this region.

Recently Suzuki and Sambongi (*11*) published a comprehensive high temperature EMF study of the Ti–O system. Using a variety of reference electrodes they obtained very accurate pO_2-composition isotherms. Their results for the Magnéli phase regions at 1473°K are reproduced by the solid line in Fig. 3. There is good agreement between their results and the mean of our oxidation/reduction results. In their work Suzuki and Sambongi made no reference to hysteresis; their samples were prepared by direct combination of Ti metal with TiO_2 under vacuum. The results of Suzuki and Sambongi also show narrower homogeneity ranges for the *n*-odd homologues compared to those for the *n*-even homologues, in agreement with our results.

For the Magnéli phases in contact with metallic iron the data in Fig. 4 show considerable reduction in the magnitude of both the hysteresis effect and the bivariant behaviour compared with those observed in the binary system.

As with the Ti–O system, the *n*-odd single phase homologues containing iron showed narrower homogeneity regions than the adjacent *n*-even homologues. In a parallel study on the Mn–Ti–O system we have observed that manganese completely destabilizes

the *n*-odd homologues, and the only stable Magnéli phases are $(Ti, Mn)_4O_7$, $(Ti, Mn)_6O_{11}$ and $(Ti, Mn)_8O_{15}$.

At 1473°K each of the phases incorporate iron from 1.2 at.% iron in M_8O_{15} to 0.8 at.% iron in M_3O_5 (Table III and Fig. 5). From Mössbauer studies on ^{57}Fe-enriched iron doped phases we have determined that, as expected, the incorporated iron is divalent (*18*), i.e., there is partial solid solution between each of the titanium oxide phases Ti_nO_{2n-1} and the hypothetical ferrous iron counterparts $FeTi_{n-1}O_{2n-1}$. From Table III and Fig. 5 the limits for the M_8O_{15} and M_4O_7 solid solutions are calculated as $(FeTi_7O_{15})_{0.096}(Ti_8O_{15})_{0.904}$ and $(FeTi_3O_7)_{0.040}(Ti_4O_7)_{0.960}$; i.e., almost 10% of the trivalent titanium in M_8O_{15} is replaced, $2Ti^{3+} \equiv Fe^{2+} + Ti^{4+}$. This replacement falls in the lower Magnéli phases to less than 4% in M_4O_7. Marezio and Dernier (*19*) have shown that in Ti_4O_7 the trivalent titanium is randomly distributed between the rutile slabs and shear slabs. Mössbauer studies show a preferential incorporation of Fe^{2+} in the rutile slabs (*20*).

Application to Ilmenite Upgrading

In one of the more promising ilmenite upgrading methods (*2*) (operated by the company Western Titanium N.L. in Western Australia) ilmenite is reduced at 1473°K in an atmosphere produced by the partial combustion of coal with resulting oxygen activities of 10^{-15}–10^{-16}. The reduction product consists of metallic iron and titanium-rich oxide phases, containing ~70% by weight of reduced rutiles. Kiln conditions approximate to equilibrium isothermal reduction because of the high temperature involved and the long residence times. For such products and conditions the data presented in Figs. 4 and 5 and Table III can be used to determine the amount of iron retained as ferrous oxide in the Magnéli phases. This iron is unattacked in the leaching stage and thus remains as an impurity in the final product. Our results show that over the whole range of oxygen activities between 10^{-15} and ~10^{-17}, the maximum incorporation of iron in the Magnéli phases is no greater than 1% by weight at 1473°K. The oxygen activity–composition isotherm of Fig. 4 may also be used, in conjunction with X-ray diffraction of the Magnéli phases produced (*14*), as a monitor of the reducing atmosphere in the commercial kiln.

References

1. H. H. Henn and J. A. Barclay, *U.S. Bur. Mines Inform. Circ.* 8450 (1970).
2. B. F. Bracanin, P. W. Cassidy, J. M. Mackay, and H. W. Hockin, *TMS Paper Selection No. A72–31*, 209–259 (1972).
3. I. E. Grey and A. F. Reid, Reaction sequences in the reduction of ilmenite. 3. *Inst. Mining Met. Trans., Sect. C*, **83**, 39 (1974).
4. I. E. Grey, A. F. Reid, and D. G. Jones, Reaction sequences in the reduction of ilmenite. 4. *Inst. Mining Met. Trans., Sect. C*, June 1974 (in press).
5. N. I. Bogdanova, G. P. Pirogovskaya, and S. M. Ariya, *Russ. J. Inorg. Chem.* **8**, 401 (1963).
6. V. Porter, Ph.D. Thesis, Pennsylvania State University (1965).
7. P. G. Wahlbeck and P. W. Gilles, *J. Amer. Ceram. Soc.* **49**, 180 (1966).
8. J. S. Anderson and A. S. Khan, *J. Less-Common Metals* **22**, 219 (1970).
9. R. R. Merritt, Ph.D. Thesis, University of Western Australia (1970).
10. R. R. Merritt, B. G. Hyde, L. A. Bursill, and D. K. Philp, *Phil. Trans. Roy. Soc. London, Ser. A*, **274**, 627 (1973).
11. K. Suzuki and K. Sambongi, *Tetsu To Hagane* **58**(12), 1579 (1972).
12. A. H. Webster and N. F. H. Bright, *J. Amer. Ceram. Soc.* **44**, 110 (1961).
13. L. S. Darken and R. W. Gurry, *J. Amer. Chem. Soc.* **67**, 1398 (1945).
14. S. Andersson, B. Collen, U. Kuylenstierna, and A. Magnéli, *Acta Chem. Scand.* **11**, 1641 (1957).
15. A. Levy, *J. Sci. Instrum.* **41**, 449 (1964).
16. J. S. Anderson and R. J. D. Tilley, *J. Solid State Chem.* **2**, 472 (1970).
17. B. G. Hyde, D. J. M. Bevan, and L. Eyring, *Phil. Trans. Roy. Soc. London, Ser. A*, **259**, 583 (1966).
18. I. E. Grey and J. Ward, *J. Solid State Chem.* **7**, 300 (1973).
19. M. Marezio and P. D. Dernier, *J. Solid State Chem.* **3**, 340 (1971).
20. I. E. Grey and J. Ward, unpublished.